ORIGINAL ARTICLE

CrossMark

Assessment of the thermal response of variations in land surface around an urban area

Mojolaoluwa Toluwalase Daramola[1] · Emmanuel Olaoluwa Eresanya[1,2] · Kazeem Abiodun Ishola[1,3]

Abstract

The ancient city of Ibadan has experienced major development and this development has led to modifications of the land surface over the years. This study assessed the changes that have occurred in the Land Use Land Cover (LULC) of Ibadan city using satellite image from Landsat covering 1984, 2000 and 2016. Supervised classification scheme was done using the maximum likelihood classifier for classifying the images. The extent of change of the LULC classes was performed on the classified images using Land Change Modeller (LCM). The implication of the change in LULC on Land Surface Temperature (LST) and related indices was assessed. Over a period of 32 years (1984–2016), the area coverage of the built-up region of Ibadan increased from 11.23 to 54.64 hectares in thousands with a net change of 8%. Thick vegetation was identified as the major contributor to the increase in the built-up area thus indicating urban encroachment. The implication of this was observed in thermal hotspots distribution and increase in the average LST over Ibadan as there was a decrease in vegetated surfaces that dampen the LST and an increase in the impervious surface revealed by the impervious and built-up index. In general, this study showed the capability of impervious surface indices in depicting the variations in land use land cover around a region, majorly urban sprawl. Furthermore, the evaluation of the spectral indices showed Urban Index (UI) as the best predictor LST.

Keywords Land cover change · Impervious surface · Land surface temperature · Population · Spectral indices

Introduction

The biophysical environment is severely modified by the variations that occur in land use land cover. These variations include; decrease in naturally vegetated area such as highly forested areas, loss of agricultural lands, increase in barren areas, increase in impermeable surfaces, etc. A major land use that has expanded over time is the impervious surfaces. Impervious surfaces are typically described as land surface features created by humans through which water cannot permeate the ground. Human-induced land cover amount to nearly 40% of the earth's surface and the naturally vegetated environments have been modified to impervious surfaces (Sterling and Ducharne 2008). Impervious surfaces are significant pointers to the state of the environment inasmuch as they have substantial consequences for several biophysical processes such as urban heat islands effect, surface energy budget, transport of water pollutants and deterioration of water quality. Impervious surfaces cause increased storm water runoff which consequently increases floods in urban streams (Rose and Peters 2001; Burns et al. 2005). As a result of the replacement of the land cover with impervious surfaces which give rise to reduction of evapotranspiration (Carlson 1986), and therefore sensible heat flux increase, temperature gradient exists between the areas dominated by impervious surfaces and natural vegetation.

Across various cities globally, studies have revealed that the proportion of green areas that should be preserved, are being urbanized (Rosenzweig et al. 2006; Kim and Pauleit 2007; Qiao et al. 2013; Kandel et al. 2016). Depletion of these green areas may result to deprivation and reduction in the biodiversity and consequently distort the urban ecosystem (Kim and Pauleit 2007). Due to the importance of urban

✉ Mojolaoluwa Toluwalase Daramola
daramolamt@futa.edu.ng

[1] Department of Meteorology and Climate Science, Federal University of Technology, P.M.B. 704, Akure, Nigeria

[2] Department of Marine Science and Technology, Federal University of Technology, P.M.B. 704, Akure, Nigeria

[3] Department of Geography, National University of Ireland, Maynooth, Ireland

areas, it is very important to give a quantitative analysis in order to describe and forecast some problems that have occurred in the process of urbanization.

The Land is the portion of the earth's terrestrial surface, comprising all attributes of the biosphere immediately above/below it (FAO 1995) and the increasing demand of man calls for optimal and proper utilization of land which can be achieved only through the proper land use/land cover study. Assessment of the land use land cover dynamics is effective in the conservation of land resources, it helps to promote economic development as well as enhance eco-friendly planning and sustainable environmental growth (Choudhari 2013). This has resulted in a global focus on the changing patterns of land use land cover at the regional scale and attention has been drawn to its implication on the biophysical environment for different regions. Some studies have focused on the thermal response of an urban setting to vegetation presence (Zhang et al. 2009; Nie et al. 2016). For instance, Zhang et al. (2013), investigated the changing landscape patterns of land cover over Sydney and its effect on the land surface temperature. In Beijing City, China, the land use changes and the corresponding variation in surface temperature were assessed by Ding and Shi (2013); in English Bazar and Jharkand, India, the changes in land surface temperature as a result of land use land cover alteration was presented by Pal and Ziaul (2017) and Kayet et al. (2016) respectively. A mutual inference from these works was the changing pattern of impervious surfaces due to urbanization over the regions and the effect on the land surface temperature.

Development of urban areas like in most cities of the world is also occurring in various parts of Nigeria. With particular focus on urban expansion, studies have been carried out in examining the changes in land use land cover in several cities across Nigeria (Musa et al. 2012; Mmom and Nwagwu 2013; Jibril and Liman 2014; Daramola and Eresanya 2017). The implication of modified biophysical features on the thermal environment has also been reported recently in some parts of Nigeria (Adeyeri and Okogbue 2014; Ishola et al. 2016a; Ige et al. 2017; Adeyeri et al. 2017; Ogunjobi et al. 2018).

The progress in remote sensing technology has resulted in the development of several indices applicable in urban impervious surface studies, some of which include; Urban Index (UI) (Kawamura et al. 1996), Normalized Difference Built-up Index (NDBI) (Zha et al. 2003), Index-based Built-up Index (IBI) (Xu 2008), New Built-up Index (NBI) (Jieli et al. 2010), Enhanced Built-up and Bareness Index (EBBI) (As-syakur et al. 2012) and Normalized Difference Impervious Index (NDII) (Wang et al. 2015). These indices have been applied in studies globally (Basarudin and Adnan 2014; Bouzekri et al. 2015; Mushore et al. 2017; Badlani et al. 2017).

These indices are useful for characterizing and extracting the features of the urban surface areas and hence can be applied for examining the variations in impervious surfaces. Arnold and Gibbons (1996) stated that variations in impervious surface areas are significant indicators of environmental change in a city. This, therefore, elucidates the importance of assessing the variations in impervious surfaces around a region. At the moment, however, only a few studies have applied the use of impervious and built -up indices in characterizing the land surface features for any area in Nigeria. Only recently, the Normalized Vegetation Built-up Index was employed by Ishola et al. (2016b) over Abeokuta and Adeyeri et al. (2017) over Abuja. Previous study over Ibadan by Akintola (1994), revealed the increase in the impervious surface within the area between 1965 and 1994. Kamdoum et al. (2014) also investigated the variation of impervious surface between 1984 and 2006. However, no study at present provides information on the current impervious surface coverage in Ibadan.

Urban areas in Nigeria are presently confronted with upsurge in population which is rapidly growing coupled with poor infrastructure across the urban areas (Ayanlade 2016). According to the United Nations report (UN 2012), the population of Nigerian cities are expected to increase in the next 40 years, consequently increasing the pressure on the land resulting to urban expansion. The city of Ibadan has experienced tremendous population increase and infrastructural development over the past few decades. With the increase in the population of Ibadan, there is need to assess the changes in the land use land cover that have occurred over time. This study thus focuses primarily on investigating the changes in the land surface features that have occurred over Ibadan for three different time periods and the corresponding thermal variation within these periods. In view of this, several impervious surface indices were applied in the study to assess the variation in land use land cover. The variation in land surface temperature was also assessed with respect to changing land use land cover pattern and structure; and finally, the assessment of these indices as land surface temperature predictors was carried out.

Study area

This research focused on the city of Ibadan, located within latitudes 7°05′0″N and 7°45′0″N and longitudes 3°30′0″E and 4°10′0″ E (Fig. 1). Ibadan is the capital of Oyo State, a state located in the south-western part of Nigeria. The climate of Ibadan is tropical and is influenced majorly by trade winds, South-West and North-East trade winds. The North-East trade winds bring about the dry season over the area and it is usually dry and dusty, whereas, during the wet season period, South-Western trade winds are prevalent over
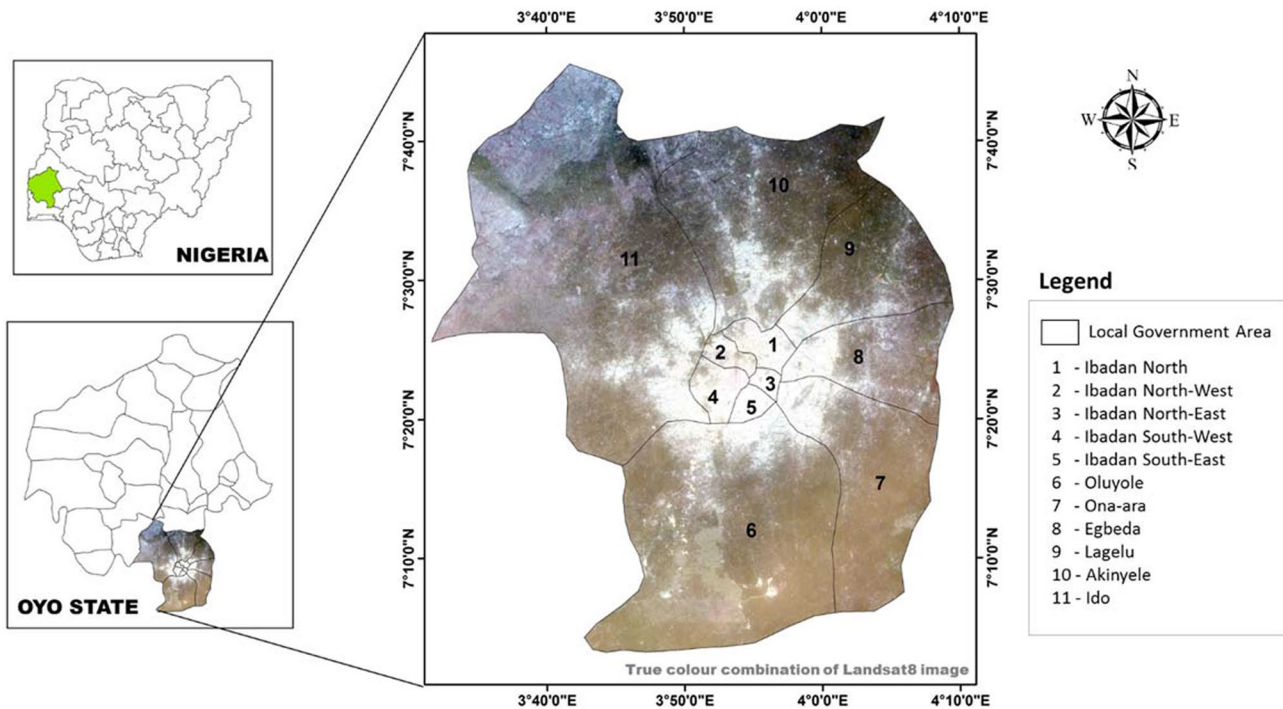
Fig. 1 Location of Ibadan, showing the local government areas

the area. The annual rainfall over Ibadan is about 1252 mm, the annual minimum and maximum temperatures are 23 and 32 °C respectively, while the average relative humidity is about 76%. It falls within the tropical rainforest and has an average elevation of 233 m. The population of Ibadan was 1,835,300 in 1991 and has witnessed remarkably increase since then with the population reaching 2,559,853 in 2006.

Materials and methods

Cloud-free remotely sensed data from Landsat were used in this study. The Landsat data were obtained from the United States Geological Survey (USGS) for 1984, 2000 and 2016 covering a period of 32 years (Table 1). The Landsat images were obtained from Landsat TM, ETM + and OLI/TIRS sensors. The acquired images were obtained for path 191 and row 55, which sufficiently covered the whole city of Ibadan. The city of Ibadan was subdivided into eleven zones

representative of the local government boundaries. Population data was also obtained from the National Population Commission (NPC).

The acquired images were processed and geometrical correction was carried out on the images. The images were referenced to the Universal Transverse Mercator (UTM) Zone 31 North and projected to World Geodetic System (WGS) 84. A classification scheme was developed for image classification (Table 2). The classification scheme was developed based on the features and knowledge of the study area. Different band combinations were produced for the images in order to adequately capture the land use land cover classes. Supervised classification was carried out on the images by applying the classification scheme. Maximum likelihood parametric rule, which has been identified as the most extensively utilized parametric classification algorithm (Jensen 2005b; Bailly et al. 2007), was adopted for the image classification. Maximum Likelihood decision rule is based on the possibility that a pixel belongs to a specific class. The basic equation (Eq. 1) assumes

Table 1 Satellite image used for this study

Satellite	Sensor	Path	Row	Source	Date acquired	Resolution (m)
Landsat5	TM	191	55	USGS	18th December, 1984	30 120 (30)
Landsat7	ETM+				6th February, 2000	30 60 (30)
Landsat8	OLI/TIRS				2nd February, 2016	30 100 (30)

Table 2 Classification scheme used in the study

Land use land cover class	Description
Barren land	Bare surface with no vegetation, open land
Scattered vegetation	Open grassland with sparse shrubs mixed with bare soil
Thick vegetation	Forested areas, densely vegetated areas, trees
Water body	Lakes, rivers, reservoirs, ponds
Light vegetation	Grassland, crops, gardens, parks, agricultural lands
Built-up	Urban settlement, residential, commercial, industrial areas

that these possibilities are equal for all classes and that the input bands have normal distributions (Erdas 1999).

$$D = \ln\left(a_c\right) - \left[0.5\ln\left(|cov_c|\right)\right] - \left[0.5\left(X - M_c\right)T\left(cov_c^{-1}\right)\left(X - M_c\right)\right] \tag{1}$$

where D is weighted distance (likelihood), c is a particular class, X is measurement vector of the candidate pixel, M_c is the mean vector of the sample of class c, a_c is percent probability that any candidate pixel is a member of class c, Cov_c is covariance matrix of the pixels in the sample of class c and T is the transposition function (matrix algebra).

Upon producing the Land Use Land Cover (LULC) maps, the Land Change Modeller (LCM) was employed for change detection analysis. Change detection analysis is a procedure applied for quantifying changes in land use land cover types produced by geographically referenced dataset of various time periods (Ramachandra and Kumar 2004). Change detection was done using the land use land cover maps for; 1984–2000 and 2000–2016, a 16-year period between each and 32-year period (1984–2016). The Land Change Modeller used, is an integrated software within the Idrisi environment that enables researchers to assess the changes in land cover between two different time periods. The requirement for LCM is basically two maps of different time periods with the same spatial characteristics and reference. LCM was applied for the identification and quantification of the changes and transitions between land cover types that occurred over different time periods. The gains and losses between each land cover, net change in land cover areas and the relative contributions of each land cover type to the net change in the area of the land use types for each time period were performed.

The overall classification accuracy (Eq. 2) and the kappa coefficient (Eq. 3) (Bogoliubova and Tymków 2014; Congalton 1991) were obtained for the classified images by generating 150 equalized random points, this was then compared to the referenced data. The kappa coefficient ranges between 0 and 1, the closer the value is to 1, the better the agreement between the dataset.

$$T = \frac{\sum D_{ii}}{N} \tag{2}$$

$$k = \frac{N \sum_{i=1}^{r} x_{ii} - \sum_{i=1} r(x+i) * (x+i)}{N^2 - \sum_{i=1}^{r} r(x+i) * (x+i)}, \tag{3}$$

where D_{ii} is the number of correctly classified pixels, N represents all the pixels in matrix error, r is the number of rows in the error matrix, x_{ii} is the number of observations in the ith row and column, $(x+1)$ is the total number of observations in the ith column and N is the total number of observation sites.

The flowchart for this study is shown in Fig. 2.

Land surface temperature (LST) estimation

The land surface temperature for each of the images was computed from the thermal band of each image. The digital number (DN) of the images were first converted to spectral radiance (L_λ) using Eq. 4.

$$L_\lambda = \left(\frac{LMAX - LMIN}{QCALMAX - QCALMIN}\right) * (DN - QCALMIN) + LMIN. \tag{4}$$

where; DN is the digital number of each pixel, LMAX and LMIN are calibration constants, QCALMAX and QCALMIN are the highest and lowest range of values for rescaled radiance in DN obtained from the metadata.

The spectral radiance was further converted to At-sensor brightness temperature (T_B) (Eq. 5).

$$T_B = \frac{K_2}{ln\left(\frac{K_1}{L_\lambda} + 1\right)} \tag{5}$$

where K_1 and K_2 are calibration constants for the landsat image given as $K_1 = 607.76$, 666.09 and 774.89, while $K_2 = 1260.56$, 1282.71 and 1321.08 (Wm^{-2} sr^{-1} μm^{-1}) for landsat TM, ETM + and OLI/TIRS respectively; L_λ is the spectral radiance for the thermal band.

After obtaining the brightness temperature, the land surface temperature was computed using Eq. 6.

$$LST_K = \frac{T_B}{1 + \left[\frac{\lambda * T_B}{\rho}\right] * \ln \varepsilon} \tag{6}$$

where T_B is the brightness temperature from Eq. 5, λ is the wavelength of emitted radiance which equals 11.5 μm, ρ is 1.438×10^{-2} mK, and ε is the emissivity.

Fig. 2 Flowchart for the study
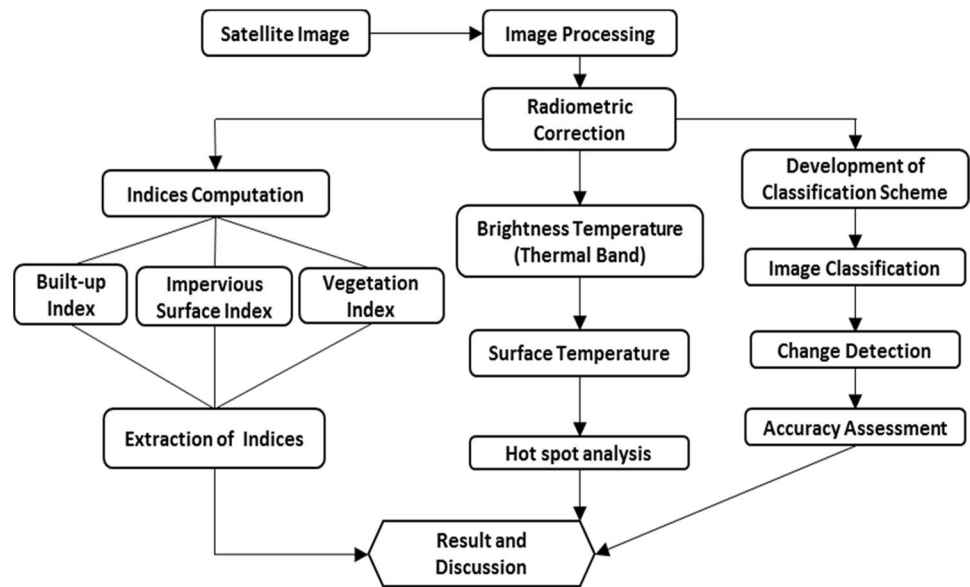
Equation 6 gives the LST in Kelvin and therefore was converted to Celsius according to Eq. 7.

$$LST_c = LST_K - 273.14 \tag{7}$$

where LST_K is the land surface temperature obtained from Eq. 6.

Thermal hot and cold spots were identified for the study region. Getis–Ord G_i^* (Getis and Ord 1992; Ord and Getis 1995), a geostatistical tool was used for identifying statistically significant hot and cold spot concentration.

$$G_i^* = \frac{\sum_{j=1}^{n} w_{i,j} x_j - \bar{X} \sum_{j=1}^{n} w_{i,j}}{S\sqrt{\left[n \sum_{j=1}^{n} w^2_{i,j} - \left(\sum_{j=1}^{n} w_{i,j}\right)^2\right]/(n-1)}} \tag{8}$$

$$\bar{X} = \frac{\sum_{j=1}^{n} x_j}{n} \tag{9}$$

$$S = \sqrt{\frac{\sum_{j=1}^{n} x_j^2}{n} - \left(\bar{X}\right)^2}. \tag{10}$$

where x_i is the attribute value for feature j, $w_{i,j}$ is the spatial weight between feature i and j, n is the total number of sample points.

Spectral Indices

A few spectral indices were utilized in this study to characterize and assess the changes in the land surface features. The impervious surface indices used were; Urban Index (UI) (Kawamura et al. 1996), Normalized Difference Built-up Index (NDBI) (Zha et al. 2003), Index-based Built-up Index (IBI) (Xu 2008), New Built-up Index (NBI) (Jieli et al. 2010), Enhanced Built-up and Bareness Index (EBBI) (As-syakur et al. 2012) and Normalized Difference Impervious Index (NDII) (Wang et al. 2015). UI (Eq. 11), exploits the inverse relationship between the brightness of urban areas in near infrared (0.76–0.90 μm) and mid-infrared (2.08–2.35 μm) portions of the spectrum (Kawamura et al. 1996). NDBI (Eq. 12), which works with the assumption that the spectral reflectance of urban areas in TM5 exceeds that in TM4 maps the built-up areas within a region of interest. It was computed from the short-wave infrared (SWIR1) and near-infrared (NIR) band (Zha et al. 2003). The IBI applies the use of thematic Index-derived bands to construct an index rather than by the original image bands (Xu 2008) and was computed using Eq. 13. NBI (Eq. 14), takes advantage of the spectral response of the red, shortwave infrared and near-infrared bands for extraction of built-up areas (Jieli et al. 2010). EBBI (Eq. 15), applies the wavelengths of near infrared, shortwave infrared and thermal infrared bands for built-up and bare land extraction, based on the characteristics of built-up and bare land areas (As-syakur et al. 2012). NDII is an index developed by Wang et al. (2015) for estimation and extraction of urban impervious surface areas. It was computed from the visible (Vis) and thermal (TIR) band (Eq. 16).

Vegetative indices, Normalized Difference Vegetation Index (NDVI) (Tucker 1979), Soil Adjusted Vegetation Index (SAVI) (Huete 1988) and Enhanced Vegetation Index 2 (EVI2) (Jiang et al. 2008) were also applied. NDVI (Eq. 17) which signifies vegetation health was computed from the near-infrared (NIR) and red band of the reflectivity. It differentiates well-vegetated areas from

less vegetated areas. NDVI values are from -1 to $+1$ and low values (negative values) implies poor vegetation health which usually occurs around less vegetated areas while high values (positive values) implies vegetation abundance. SAVI (Eq. 18), was modified from NDVI as a result of the influence of soil brightness due to low vegetation cover (Huete 1988). EVI2 (Eq. 19), was developed by decomposing the Enhanced Vegetation Index (Liu and Huete 1995) into a 2-band EVI by relating the blue band to the red band (Jiang et al. 2008).

$$UI = \frac{SWIR2 - NIR}{SWIR2 + NIR} \qquad (11)$$

$$NDBI = \frac{(SWIR1 - NIR)}{(SWIR1 + NIR)} \qquad (12)$$

$$IBI = \frac{\frac{2*SWIR1}{SWIR1+NIR} - \left[\frac{NIR}{NIR+RED} + \frac{GREEN}{GREEN+SWIR1}\right]}{\frac{2*SWIR1}{SWIR1+NIR} + \left[\frac{NIR}{NIR+RED} + \frac{GREEN}{GREEN+SWIR1}\right]} \qquad (13)$$

$$NBI = \frac{RED * SWIR1}{NIR} \qquad (14)$$

$$EBBI = \frac{SWIR1 - NIR}{10 * \sqrt{(SWIR1 + TIRS)}} \qquad (15)$$

$$NDII = \frac{(Vis - TIR)}{(Vis + TIR)} \qquad (16)$$

$$NDVI = \frac{(NIR - RED)}{(NIR + RED)} \qquad (17)$$

$$SAVI = (1 + L) * \frac{(NIR - RED)}{NIR + RED + L} \qquad (18)$$

$$EVI2 = 2.5 \frac{NIR - RED}{NIR + 2.4 * RED + 1} \qquad (19)$$

In examining the relationship between the spectral indices and land surface temperature, statistical analysis was performed. Correlation between the land surface temperature and spectral indices was examined which revealed the spectral index with the strongest correlation with land surface temperature. The index was then used for estimation of land surface temperature using linear regression model. Statistical measures which include Root Mean Square Error (RMSE), Coefficient of Efficiency (COE) and the Index of Agreement (IOA) were employed for evaluating the model performance.

Results and discussion

Land use land cover analysis

The Landsat images of Ibadan classified into 6 different land use land cover types (barren land, scattered vegetation, thick vegetation, water body, light vegetation and built-up) for 1984, 2000 and 2016 are shown in Fig. 3. It was observed that zones 1–5 was the major settlement area in 1984 and was the main urbanized region of the land cover, though few settlements were found in other zones. Urban sprawl was evident in 2000, as built-up increased outwards from zones 1–5 and expanded into the other surrounding zones. This represents the early stages of the development around the zones 6–11. As at 2016, further development of zones 6–11 had occurred with the further expansion of built-up from zones 1–5 to zones 6–11. The continual increase in built-up area which represents urban expansion is expected with the steady increase in the population of Ibadan (Table 3). According to the National Population Commission (NPC), the population of Ibadan has increased since 1991 (which represents years after the 1984 study period) from 1,835,300 to a projected population of 3,034,206 in 2011. The population density of each zone (Fig. 4) shows an increase in the population density of each zone but particularly, zones 1–5 were more densely populated than other zones which indicates the pressure on the land surface with increased population.

In order to reveal the changes in the land use land cover classes, the area coverage of the land cover classes was extracted for each year and plotted (Fig. 5). Thick vegetation which occupied majority of the land cover was 272.18 (hectares in thousands) in 1984, barren land, light vegetation and scattered vegetation were 22.76, 23.07 and 10.75 (hectares in thousands) while built-up was 11.73 (hectares in thousands). In 2000, thick vegetation and scattered vegetation reduced to 173.89 and 2.85 (hectares in thousands) respectively while the other land uses increased. In 2016, the area coverage of built-up increased to 54.64 (hectares in thousands). The gains and losses described what percentage of land use land cover class was converted from other classes to the land cover type and from a particular class to other land use types. The gains and losses in land cover areas (Fig. 6) showed that about 19% of the thick vegetation was converted to other land cover types from 1984 to 2000. This was the highest conversion that occurred for any land cover type for that period. About 3.5 and 2% of Light vegetation and scattered vegetation were also lost to other land use and cover types respectively. The loss in built-up and water body was relatively small compared to the other land cover types. Barren land gained the most from other land use land cover types, followed
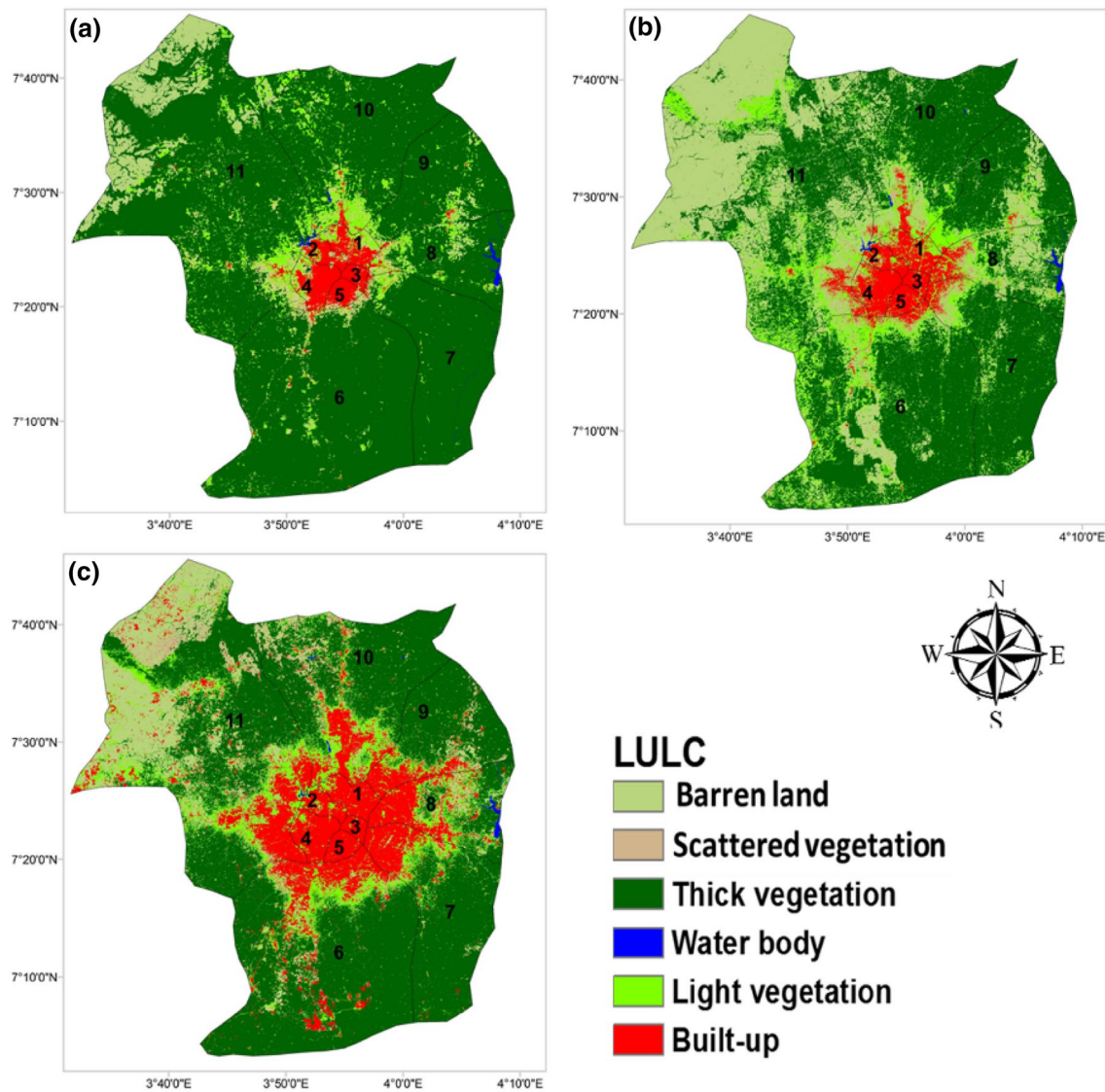
Fig. 3 Land use classification maps of Ibadan for **a** 1984, **b** 2000 and **c** 2016

by light vegetation and built-up at 14, 7 and 1.8%. From 2000 to 2016, about 11% of barren land was lost to other land cover types, 7% of light vegetation was converted to other land use types and 6% of thick vegetation was

converted to other land use types. Thick vegetation experienced the highest gain in land cover area as 8% of other land cover types were converted to it, about 7% of other land use types were lost to built-up, 5% were lost to light vegetation, 2.5% were lost to barren land and 1% was lost to scattered vegetation. The gains and losses for the land use types for 1984–2016 show that 17% of thick vegetation was lost to the other land use types which was the most compared to the other land use types. Light vegetation lost about 4%, scattered vegetation lost about 2% while barren land lost about 1%. Built-up, barren land and light vegetation gained 8, 7 and 6%, respectively. It was noted that water body experienced little variation all through the period of study. The net change in land cover area (Fig. 7) showed percentage increase of 14, 1.8 and 4%

Table 3 Total population of Ibadan

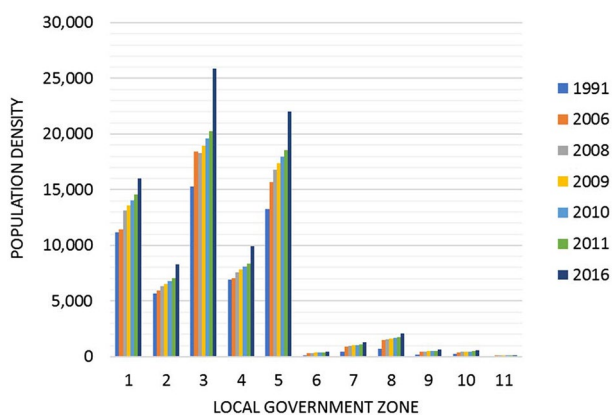| Year	Population
1991	1,835,300
2006	2,559,853
2008	2,739,977
2009	2,834,739
2010	2,932,777
2011	3,034,206

Fig. 4 Population density of each local government zone

between 1984 and 2000 for barren land, built-up and light vegetation respectively while thick vegetation and scattered vegetation decreased by 18 and 2%, respectively. Between 2000 and 2016, built-up increased tremendously by 7%, while barren land decreased significantly by 8%. The net change of thick vegetation and scattered vegetation from 1984 to 2016 were about 17% and 1.8% loss, while that of barren land, built-up and light vegetation were 6, 8 and 2.8%, respectively. Contribution to the net change in the land use land cover types between 1984 and 2016, shown in Fig. 8 revealed that thick vegetation was the highest contributor to change in built-up with 4.5% of the area converted to built-up. 1.8 and 1.2% of the light vegetation and scattered vegetation area were converted to built-up respectively, while barren land contributed 0.4% to increase in the built-up area. All the land use land cover types contributed to the increase in the area coverage of built-up except for water body which remained relatively unchanged. For the thick vegetation which occupied the

greatest area coverage of all the land use land cover types, there was conversion of portions of thick vegetation into other land use land cover classes indicated by the negative values (Fig. 8d). the largest portion of the thick vegetation area converted was to barren land with about 12% of the area converted.

The accuracy of land use land cover classification was performed on the classified images of Ibadan (Table 4). Equalized random points were generated for each classified image which was then compared with the reference data. The overall classification accuracy was 84.09, 84.48 and 83.33% for 1984, 2000 and 2016 respectively. The overall Kappa coefficient was 0.8056 for 1984 classified image, 0.8115 for 2000 classified image and 0.80 for 2016 classified image while the Kappa coefficient for the land use land cover types ranged from 0.6602 to 1.00 for all the classified images. This indicated reasonable level of classification accuracy.

Analysis of land surface temperature and spectral indices

Land Surface temperature which is a pointer to the existence of surface urban heat island (Ishola et al. 2016a) was estimated from the satellite image over Ibadan for the period of study (Fig. 9). The LST which ranged from < 22 to > 28 °C in 1984 indicated the presence of surface urban heat island within the major developed areas of zones 1–5. The highest LST existed at the urban centre with the lower surface temperatures occurring around the less populated zones. The LST for 2000 ranged between < 22 and > 29 °C. The LST of the built-up varied between 27 °C to above 29 °C, with surface urban heat island noticeable within the built-up centre also. An increase in the surface temperature around the North-West part of zone 11 between 1984 and 2000 was observed. This indicates the implication of land use

Fig. 5 Distribution of land use by area (hectares in thousand) for the study period
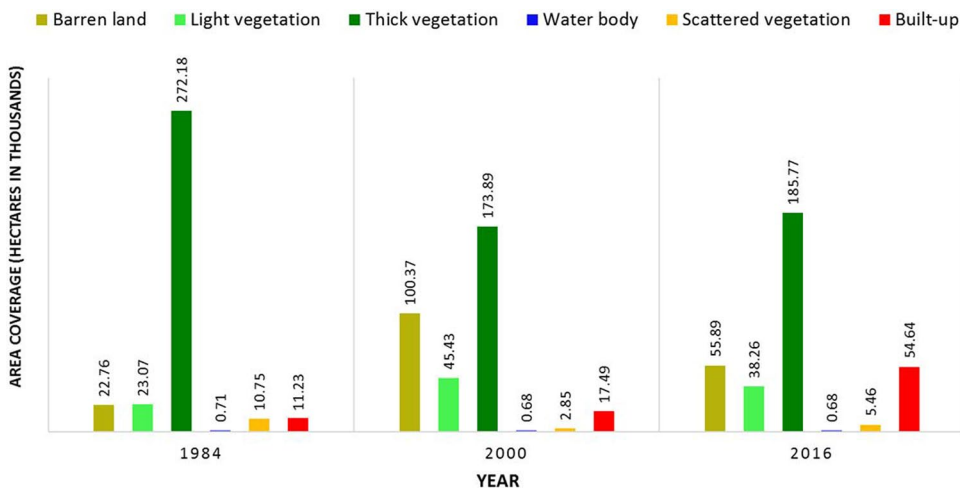
Fig. 6 Gains and losses in land cover areas by percentage between **a** 1984 and 2000 **b** 2000 and 2016 **c** 1984 and 2016
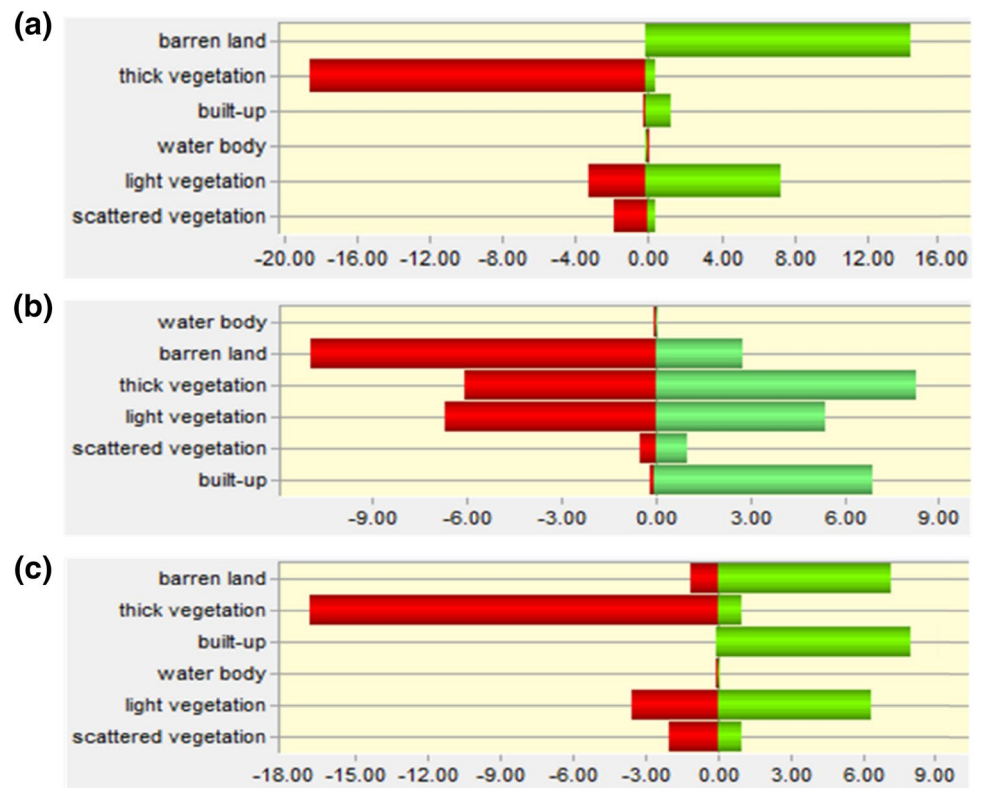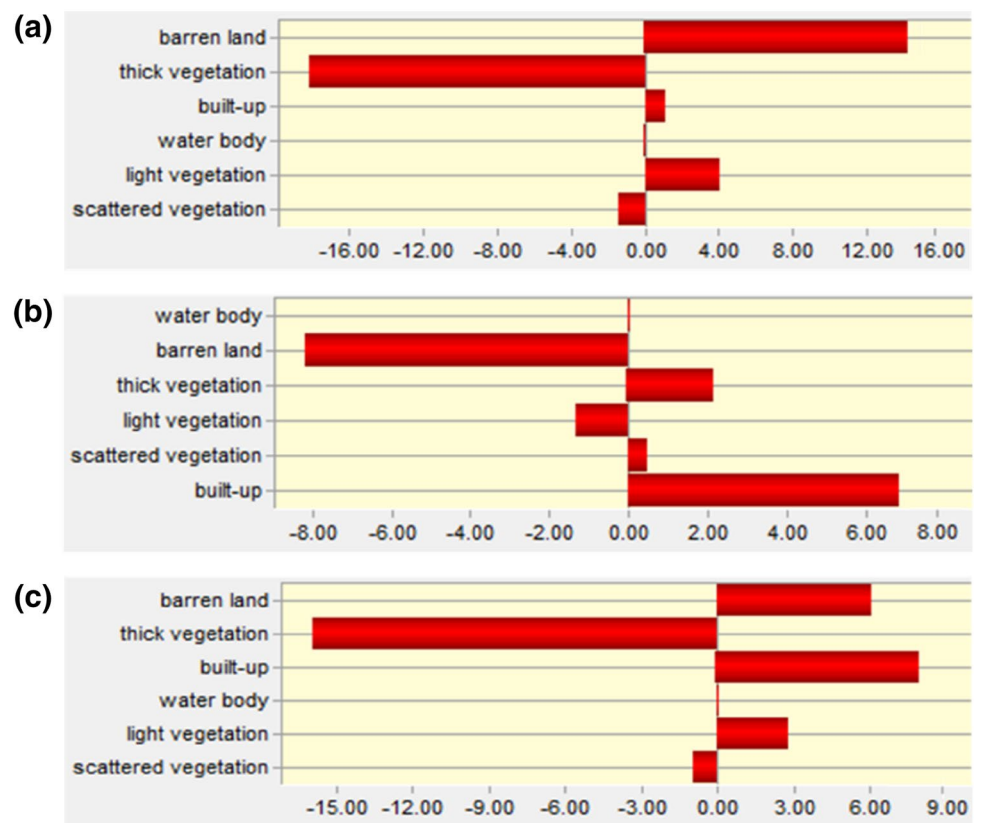

Fig. 7 Net change in land cover areas between **a** 1984 and 2000 **b** 2000 and 2016 **c** 1984 and 2016

(a)

(d)
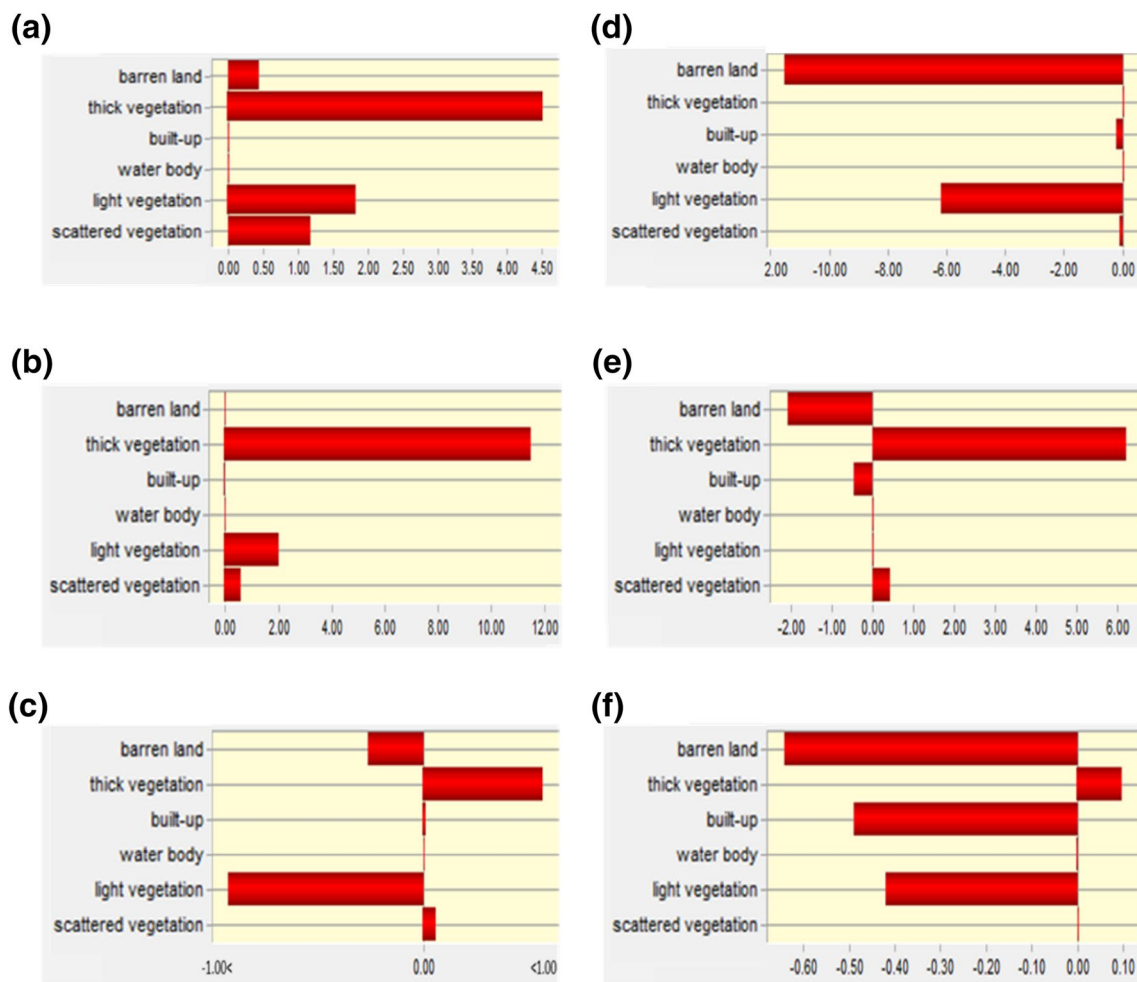

(b)

(e)

(c)

(f)

Fig. 8 Contributions to net change in **a** built-up, **b** barren land, **c** water body, **d** thick vegetation, **e** light vegetation and **f** scattered vegetation between 1984 and 2016

Table 4 Land use land cover classification assessment for each year

	1984	2000	2016
Overall classification accuracy (%)	84.09	84.48	83.33
Overall kappa statistics		0.8056	0.8115	0.80

Class name	Kappa statistics		
Barren land	0.8204	0.6979	0.8378
Light vegetation	0.6602	0.855	0.7073
Thick vegetation	0.8854	0.8117	0.7143
Water body	0.812	0.8407	1.000
Scattered vegetation	0.807	0.8568	0.8462
Built-up	0.812	0.8578	0.7073

conversion on LST as the vegetated surface in 1984 was converted to barren land. Range of LST for 2016 was 24 °C to > 29 °C. A greater part of the land surface of Ibadan

had LST range of 27 °C to > 29 °C compared to that of 1984 which ranged between 22 and 24 °C. This suggests an increase in the average LST of Ibadan from 1984 to 2016.

As stated earlier, the population increase over Ibadan particularly around the zones 1–5, resulted in a rise in the population density. This initiated more conversion of vegetative surfaces to impervious surfaces which resulted into increase in the average LST of the region. The vegetated surfaces were replaced with materials which contributed to higher LST. Similarly, the LST within the zones 6–11 increased as the impervious surface increased within the zones. Rise in LST attributable to transformation of vegetated surfaces to impervious surfaces has been identified as a crucial problem in the world today (Mallick et al. 2008). This agrees with Yuan and Bauer (2007) that stated the influence of vegetation cover on the temperature of the land surface and is observed to play a role in the development intensity of UHI (Rizwan et al. 2008; Corburn 2009; Ayanlade 2016; Sannigrahi et al. 2017). This has also been observed in studies
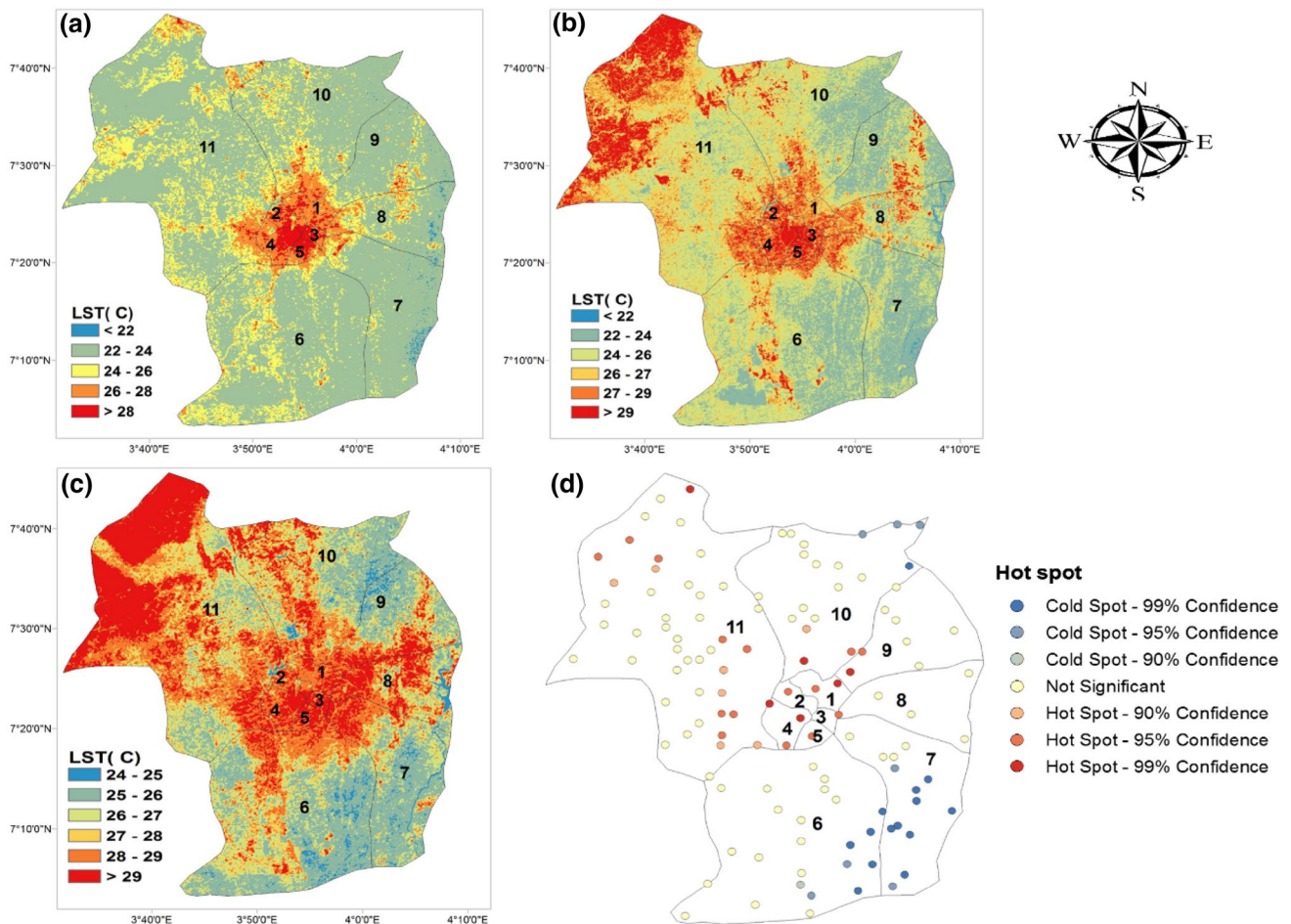
Fig. 9 Land Surface Temperature (LST) for **a** 1984, **b** 2000 and **c** 2016 and **d** hot spot maps of Ibadan

across the globe over different regions (Sahana et al. 2016; Fu and Weng 2016; Khan and Chatterjee 2016; Bokaie et al. 2016; Mushore et al. 2017; Chen et al. 2017).

Surface urban heat island was noted from the spatial distribution of the LST with higher temperatures (> 29 °C) over the built-up centre compared to the surrounding settlements. Similar to the high LST which existed around the North-West part of zone 11 in 2000, the same was noted in 2016 (> 29 °C). The land use cover over this part of zone 11 was vegetated surface in 1984 and had been converted to barren land with pockets of built-up in 2016. This shows that there exist high LST over barren land areas where there is no vegetation to reduce the surface temperature and thus reveals the effect of vegetation cover on LST damping. Hotspot analysis was also carried (Fig. 9d), indicating the area of hot spot and cold spot. The hotspots over Ibadan were noted in areas of urban built-up and also barren land areas, while the cold spots were majorly over the vegetative regions where the LST was in the range of < 26 °C. This further reveals the role played by vegetation cover and the importance in thermal cooling of an area.

The expansion of built-up over the years brings about modification of the land surface and thus has implication on the land surface features. Analysis of the land surface over Ibadan with focus on the impervious and vegetated surfaces was therefore carried out. Figure 10 shows the spatial distribution of impervious surfaces and non-impervious surfaces in 1984 over Ibadan as categorized by the different spectral indices used in this study. A similar variation of impervious surface was observed for all the indices. Nearly all the sections of zones 1–5 were categorized as impervious surfaces while the other zones were majorly non-impervious surfaces with a few impervious surfaces. More areas were categorized as built-up/impervious surface from 1984 to 2000 as revealed by Fig. 11. With the expansion in the built-up area between 1984 and 2000, there was a corresponding increase in the impervious surfaces in Ibadan. The indices clearly revealed the changes that occurred during this period as they all captured the increase in the impervious surface. Further conversion of non-impervious surface to impervious surface occurred between 2000 and 2016 as revealed by the indices (Fig. 12). The impervious surface in Ibadan increased
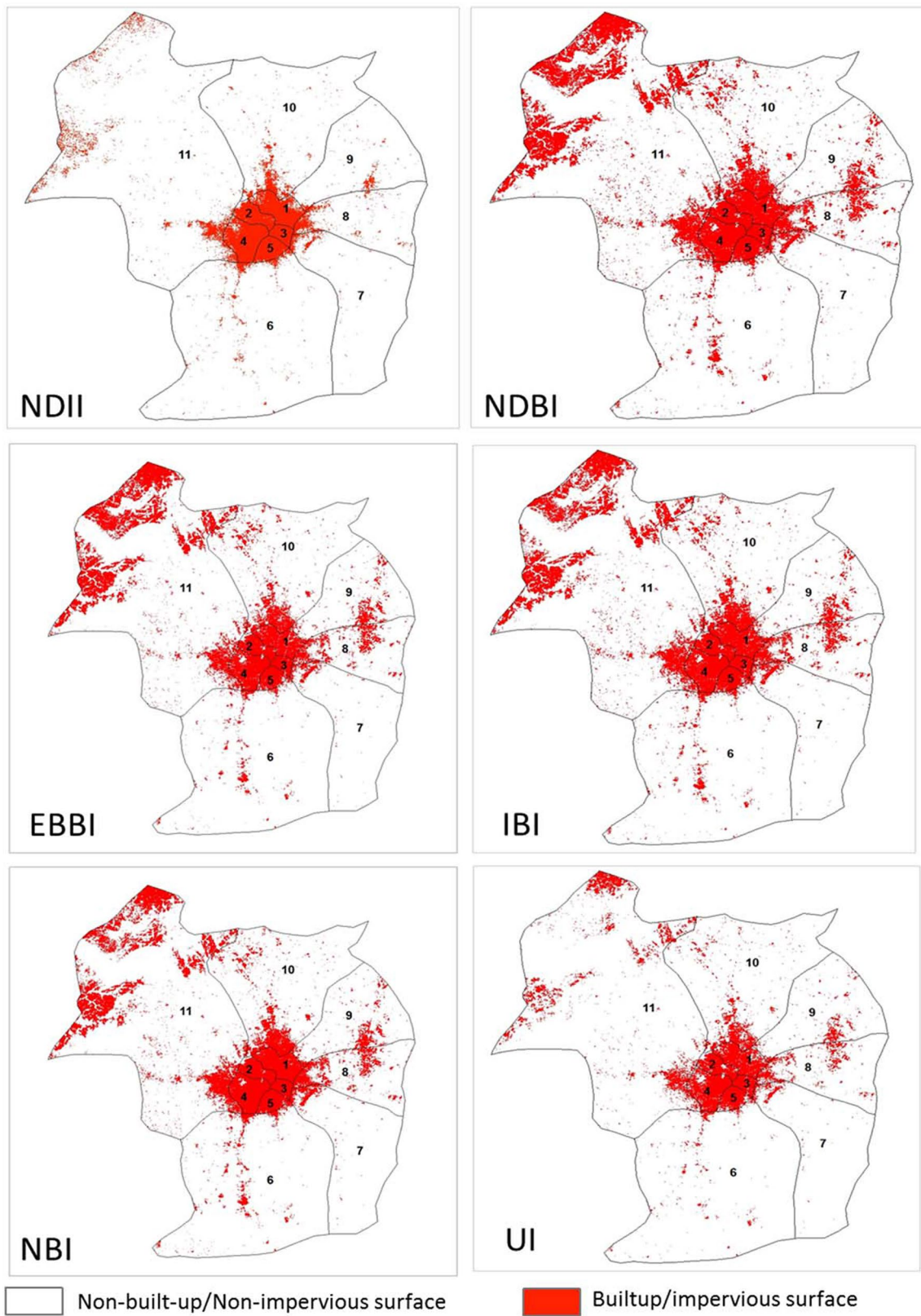
Fig. 10 Spatial distribution of the Impervious surface indices for 1984
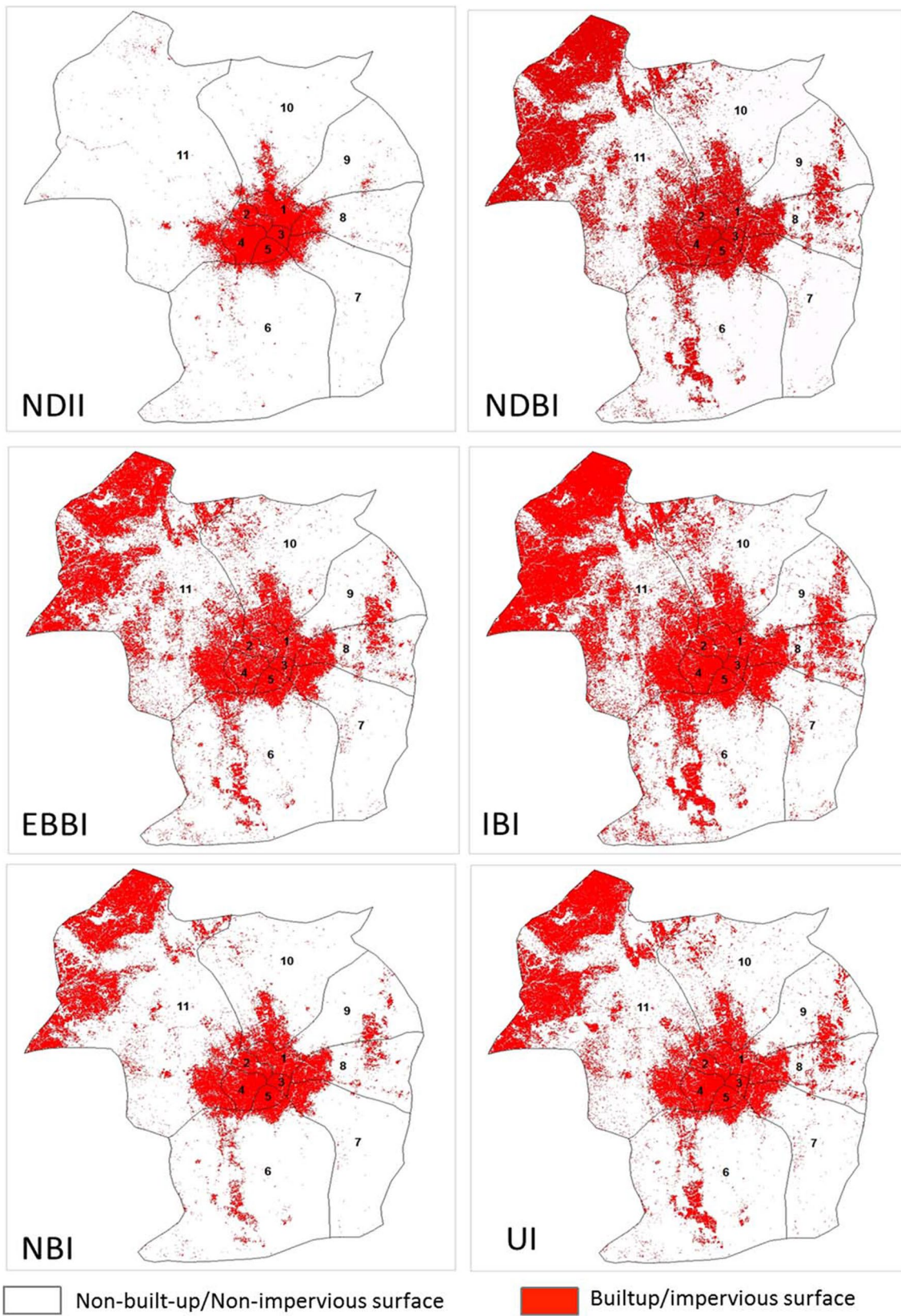
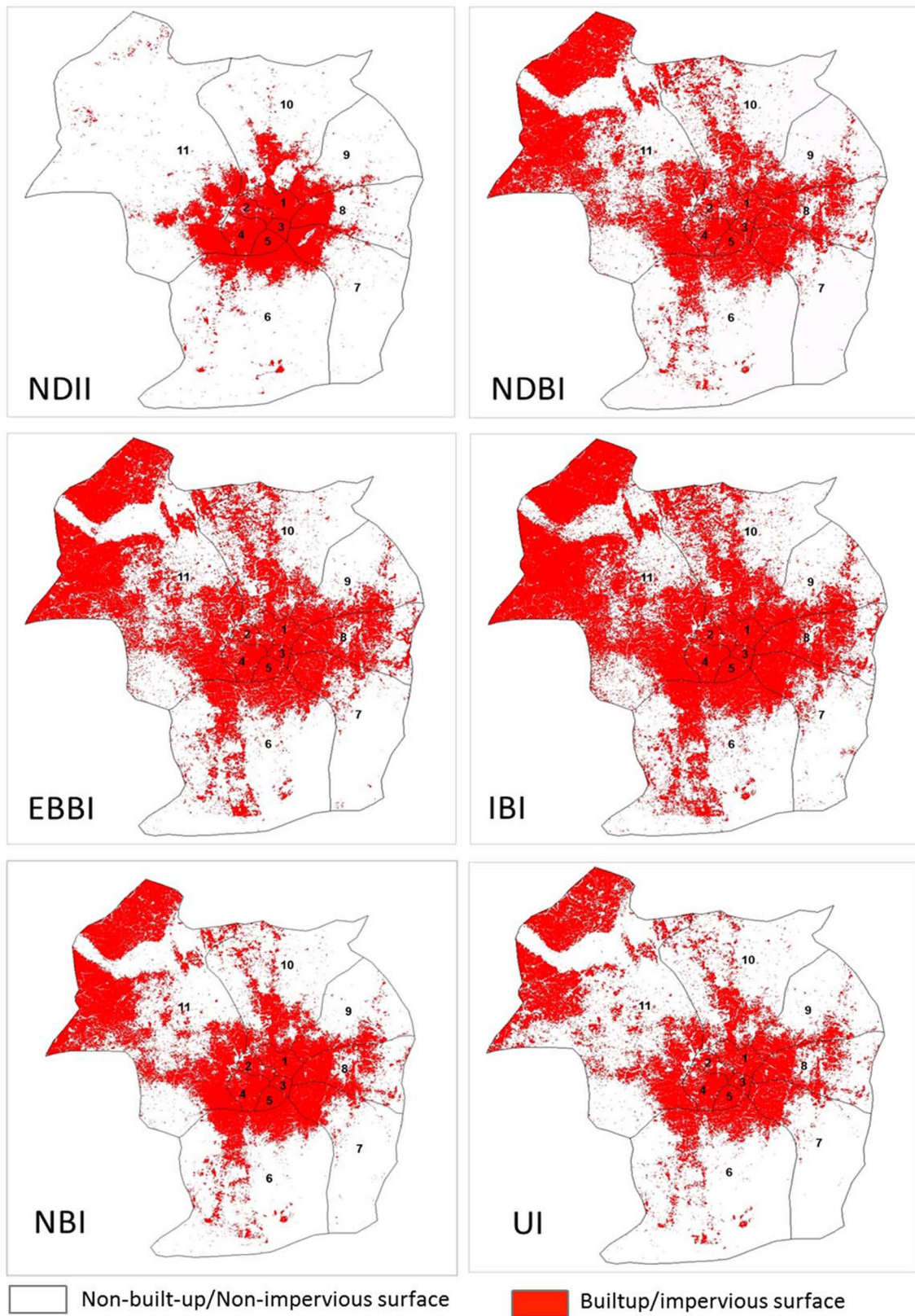**Fig. 11** Spatial distribution of the Impervious surface indices for 2000

Fig. 12 Spatial distribution of the Impervious surface indices for 2016

further, occupying a greater area coverage than the earlier years, thus indicating the increased pressure on the land surface. Increase in impervious surfaces due to urbanization was identified as a contributing factor in the 2011 flooding in Ibadan, as the impervious surfaces resulted into decreased infiltration and thus increased volume of flood flow (Agbola et al. 2012; Egbinola et al. 2017).

As mentioned earlier, the increase in impervious surface brings about modification of the land surface features which ultimately affects the surface energy budget and thus the regional climate of a region (Chakraborty et al. 2013; Ogunjobi et al. 2018). To further analyse the variation in the land surface characteristics around Ibadan, the Normalized Difference Vegetation Index (NDVI), Soil Adjusted Vegetation Index (SAVI) and Enhanced Vegetation Index 2 (EVI2) were estimated for the periods of study (Fig. 13). The vegetative surfaces were extracted denoted by the green section (vegetation), leaving the non-vegetative parts (non-vegetation). Comparing the vegetative indices with the impervious surface indices, it was noted that the non-vegetation corresponds to the impervious surfaces while the non-impervious surfaces corresponds to the vegetation. This is expected as the non-vegetation parts are the urbanized areas of Ibadan. A noticeable feature in the vegetative indices was the decrease in the vegetated surfaces and increase in the non-vegetated surfaces with time (from 1984 to 2016). As stated earlier from the land use land cover analysis, large portions of the vegetated surfaces have been modified and it was evident from NDVI, SAVI and EVI2 that conversions have been made to non-vegetated surfaces.

Regression analysis

Correlations between the LST and the spectral indices were carried out in order to examine the relationship between them (Table 5). The vegetative indices (NDVI, SAVI and EVI2) were negatively correlated with LST and the impervious surface indices all through, indicating an inverse relationship. The correlation values for LST and the vegetative indices were -0.719 for NDVI, -0.683 for SAVI and -0.724 for EVI2. For vegetative and impervious surface indices, the values ranged between -0.675 and 0.879. There was a significant positive relationship between LST and the impervious surface indices, $p < 0.05$, at 95% confidence level. All the impervious surface indices had very strong positive correlations with LST with values that ranged from 0.821 to 0.867, except for NDII that had a correlation value of 0.439. This suggests that, with the consistent high correlation between the other impervious surfaces and LST, the other indices are reasonable predictors of LST except for NDII. However, UI was used for model estimation as it was the index with the highest correlation with LST. The estimated (modelled) LST was compared with the derived

(Landsat) land surface temperature by extracting values from sample points across each LST (Fig. 14). The modelled LST showed similar distribution to that of the derived LST, with residual values ranging from -0.8 to 0.87 °C. The negative residual values represent overestimation of model while the positive residuals represent underestimation. Compared to the derived LST, the model estimation was reasonable. To further evaluate the regression model performance, statistical comparison was carried out (Table 6). The coefficient of correlation between the LSTs was 0.956 while the root mean square error was 0.354 °C. The Coefficient of Efficiency (COE) was 0.684 indicating the predictability advantage of the regression model (Legates and McCabe 1999, 2012). The Index of Agreement (IOA) was 0.842 and this indicates good model performance (Willmott et al. 2012). The general assessment of the regression model showed good model performance which therefore shows the predictability capability of UI for land surface temperature and corresponding surface urban heat island phenomenon.

Conclusion

This study examined the modifications that have occurred in the land use land cover over Ibadan city and its implication on the thermal structure of the area. Indication of anthropogenic disturbance was identified as the possible cause of the prominent changes that have occurred over time which were the loss in thick vegetation and increase in urban built-up areas. Several studies have presented the influence of man on the natural environment and this has been confirmed in this study. This information is vital in the urban planning sector and could help with future planned urbanization as majority of the urbanization process around Ibadan are unplanned. It is also important to note that this information is crucial for mitigation of the increased urbanization effect such as increased land surface temperature and development of surface urban heat island. More focus is given to clearing of thick vegetation and replacement of natural vegetative surfaces with impervious surface particularly within the urbanized regions without any consideration of the effect on the local climate of the region. Increase in the land surface temperature was noted over the period of study and this is likely to increase with further land cover changes. This hereby calls for well-planned strategies for incorporating green areas in Ibadan which will help mitigate the corresponding implication of loss of vegetation in the urbanized areas. Additionally, consideration should be given to the bioclimatic conditions over areas like Ibadan where population growth is on the continual increase. Furthermore, more attention should be given to the environmental consequences of increased impervious surfaces within the region such as susceptibility to flooding of areas dominated
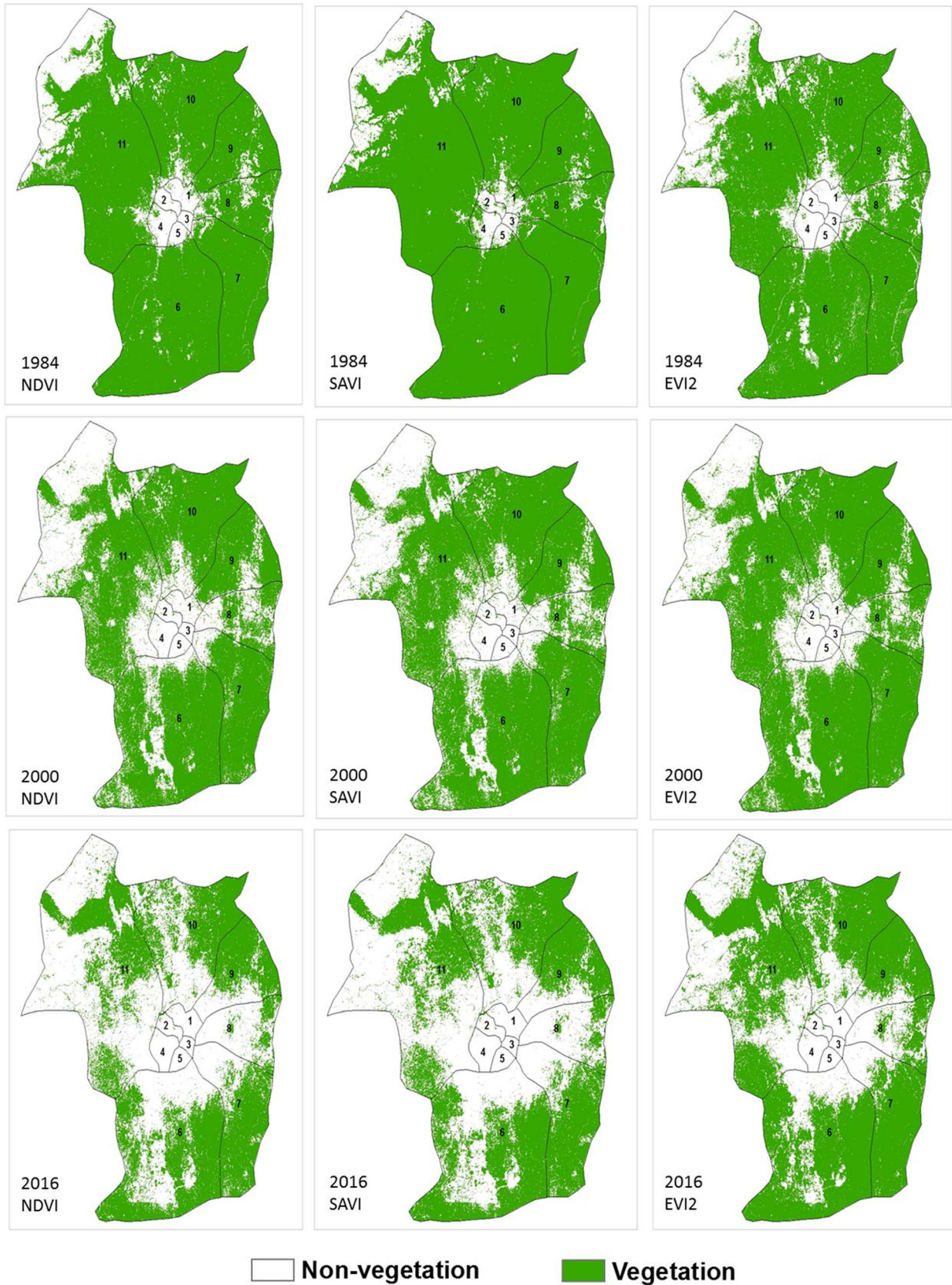
Fig. 13 Spatial distribution of the vegetative indices for 1984, 2000 and 2016

Table 5 Correlation matrix of land surface temperature and spectral indices

	NDVI	SAVI	EVI2	NDII	NDBI	EBBI	IBI	NBI	UI	LST
NDVI	1	0.993	0.998	− 0.705	− 0.829	− 0.858	− 0.813	− 0.873	− 0.868	− 0.719
SAVI	0.993	1	0.993	− 0.675	− 0.807	− 0.838	− 0.793	− 0.847	− 0.842	− 0.683
EVI2	0.998	0.993	1	− 0.708	− 0.838	− 0.861	− 0.824	− 0.879	− 0.873	− 0.724
NDII	− 0.705	− 0.675	− 0.708	1	0.582	0.570	0.563	0.767	0.662	0.439
NDBI	− 0.829	− 0.807	− 0.838	0.582	1	0.977	0.990	0.951	0.964	0.851
EBBI	− 0.858	− 0.838	− 0.861	0.570	0.977	1	0.969	0.927	0.944	0.821
IBI	− 0.813	− 0.793	− 0.824	0.563	0.990	0.969	1	0.927	0.946	0.833
NBI	− 0.873	− 0.847	− 0.879	0.767	0.951	0.927	0.927	1	0.970	0.847
UI	− 0.868	− 0.842	− 0.873	0.662	0.964	0.944	0.946	0.970	1	0.867
LST	− 0.719	− 0.683	− 0.724	0.439	0.851	0.821	0.833	0.847	0.867	1
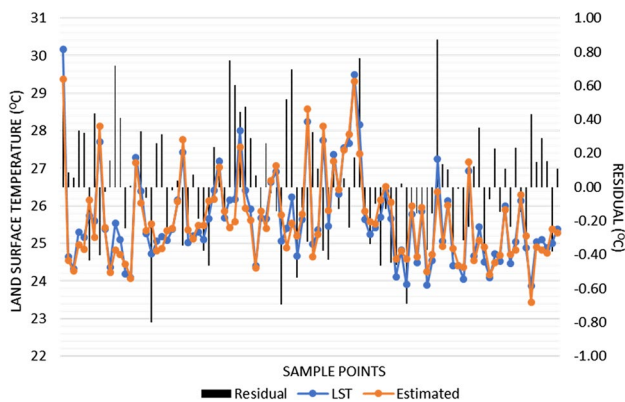
Fig. 14 Derived and regression modelled land surface temperature

Table 6 Error analysis of modelled LST

	LST
r	0.956
RMSE	0.354
COE	0.684
IOA	0.842

with impervious surfaces. With the continual increase in the population of Ibadan city, it is imperative that the land surface features be monitored due to the implication of further modification of the land use land cover.

References

Adeyeri OE, Okogbue EC (2014) Effect of landuse landcover on land surface temperature. In: Proceedings of Climate Change, and Sustainable Economic Development, pp 175–184. (**ISBN 978-978-521-43-6-9**)

Adeyeri OE, Akinsanola AA, Ishola KA (2017) Investigating Surface Urban Heat Island Characteristics over Abuja, Nigeria: relationship between land surface temperature and multiple vegetation indices. Soc Environ Remote Sens Appl. https://doi.org/10.1016/j.rsase.2017.06.005

Agbola BS, Ajayi O, Taiwo OJ, Wahab BW (2012) The August 2011 Flood in Ibadan, Nigeria: anthropogenic causes and consequences. Int J Disaster Risk Sci 3(4):207–217. https://doi.org/10.1007/s13753-012-0021-3

Akintola FO (1994) Flooding phenomenon in Ibadan region. In: Filani MO (ed) Ibadan region. Rex Charles Publications & Connel Publications, Ibadan, pp 244–255

Arnold CL, Gibbons CJ (1996) Impervious Surface coverage—the emergence of a key environmental indicator. J Am Plann Assoc 62(2):243–258. https://doi.org/10.1080/01944369608975688

As-syakur AR, Adnyana IWS, Arthana IW, Nuarsa IW (2012) Enhanced built-up and bareness index (EBBI) for mapping built-up and bare land in an urban area. Remote Sens 4:2957–2970

Ayanlade A (2016) Variation in diurnal and seasonal urban land surface temperature: landuse change impacts assessment over Lagos metropolitan city. Model Earth Syst Environ 2:193. https://doi.org/10.1007/s40808-016-0238-z

Badlani B, Patel AN, Patel K, Kalubarme MH (2017) Urban growth monitoring using remote sensing and geo-informatics: case study of Gandhinagar, Gujarat State (India). Int J Geosci 8:563–576. https://doi.org/10.4236/ijg.2017.84030

Bailly JS, Arnaud M, Puech C (2007) Boosting: A classification method for remote sensing. Int J Remote Sens 28(7):1687–1710

Basarudin Z, Adnan NA (2014) Impervious surface detection and mapping via digital remotely sensed techniques. In: International Conference on Civil, Biological and Environmental Engineering (CBEE-2014) May 27–28, 2014 Istanbul (Turkey)

Bogoliubova A, Tymków P (2014) Accuracy assessment of automatic image processing for land cover classification of St. Petersburg protected area. Acta Scientiarum Polonorum Geodesia et Descriptio Terrarum 13:1–2

Bokaie M, Zarkesh MK, Arasteh PD, Hosseini A (2016) Assessment of urban heat island based on the relationship between land surface temperature and land use/land cover in Tehran. Sustain Cities Soc. https://doi.org/10.1016/j.scs.2016.03.009

Bouzekri S, Lasbet AA, Lachehab A (2015) A New spectral index for extraction of built-up area using Landsat-8 data. J Indian Soc Remote Sens. https://doi.org/10.1007/s12524-015-0460-6

Burns D, Vitvar T, McDonnell J, Hassett J, Duncan J, Kendall C (2005) Effects of suburban development on runoff generation in the Croton River basin, New York. J Hydrol 311:266–281

Carlson TN (1986) Regional-scale estimates of surface moisture availability and thermal inertia using remote thermal measurements. Remote Sens Rev 1:197–247

Chakraborty SD, Kant Y, Mitra D (2013) Assessment of land surface temperature and heat fluxes over Delhi using remote sensing data. J Environ Manag 148:143–152. https://doi.org/10.1016/j.jenvman.2013.11.034

Chen YC, Chiu HW, Su YF, Wu YC, Chen KS (2017) Does urbanization increase diurnal land surface temperature evariation? Evidence and implications. Landsc Urban Plann 157:247–258. https://doi.org/10.1016/j.landurbplan.2016.06.014

Choudhari DK (2013) Uncertainty modeling for asynchronous time series data with incorporation of spatial variation for land use or land cover change. Thesis, Indian Institute of Remote Sensing, Dehradun

Congalton RG (1991) Remote sensing and geographic information system data integration: error sources and research issues. Photogramm Eng Remote Sens 57(6):677–687

Corburn J (2009) Cities, climate change and urban heat island mitigation: Localising global environmental science. Urban Stud 46(2):413–427

Daramola MT, Eresanya EO (2017) Land surface temperature analysis over Akure. J Environ Earth Sci 7(5):97–105

Ding H, Shi W (2013) Land-use/land-cover change and its influence on surface temperature: a case study in Beijing City. Int J Remote Sens 34(15):5503–5517. https://doi.org/10.1080/01431161.2013.792966

Egbinola CN, Olaniran HD, Amanambu AC (2017) Flood management in cities of developing countries: the example of Ibadan, Nigeria. J Flood Risk Manag 10:546–554

Erdas Field Guide (1999) Erdas Inc. Atlanta

FAO (1995) Planning for sustainable use of land resources: towards a new approach. FAO, Rome

Fu P, Weng Q (2016) A time series analysis of urbanization induced land use and land cover change and its impact on land surface temperature with Landsat imagery. Remote Sens Environ 175:205–214

Getis A, Ord JK (1992) The analysis of spatial association by use of distance statistics. Geogr Anal 24(3):189–206

Huete AR (1988) A soil-adjusted vegetation index (SAVI). Remote Sens Environ 25(3):295–309

Ige SO, Ajayi VO, Adeyeri OE, Oyekan KSA (2017) Assessing remotely sensed temperature humidity index as human comfort indicator relative to landuse landcover change in Abuja, Nigeria. Spat Inf Res 25(4):523–533. https://doi.org/10.1007/s41324-017-0118-2

Ishola KA, Okogbue EC, Adeyeri OE (2016a) A quantitative assessment of surface urban heat islands using satellite multitemporal data over Abeokuta, Nigeria. Int J Atmos Sci. https://doi.org/10.1155/2016/3170789

Ishola KA, Okogbue EC, Adeyeri OE (2016b) Dynamics of surface urban biophysical compositions and its impact on land surface thermal field. Model Earth Syst Environ 2:208. https://doi.org/10.1007/s40808-016-0265-9

Jensen J (2005) Introductory digital image processing: a remote sensing perspective, 3rd edn. Prentice Hall, Upper Saddle River

Jiang Z, Huete AR, Didan K, Miura T (2008) Development of a two-band enhanced vegetation index without a blue band. Remote Sens Environ 112:3833–3845

Jibril MS, Liman HM (2014) Land use and land cover change detection in Ilorin, Nigeria, using satellite remote sensing. J Nat Sci Res 4(8):123–129

Jieli C, Manchun L, Yongxue L, Chenglei S, Wei H (2010) Extract residential areas automatically by New Built-up Index. In: 18th International Conference on Geoinformatics, Beijing, pp 1–5 https://doi.org/10.1109/GEOINFORMATICS.2010.5567823

Kamdoum JN, Adepoju KA, Akinyede JO (2014) Assessment of impervious surface area and surface Urban Heat Island: a case study. Int J Ecol Econ Stat 35(4):48–64

Kandel H, Melesse A, Whitman D (2016) An analysis on the urban heat island effect using radiosonde profiles and Landsat imagery with ground meteorological data in South Florida. Int J Remote Sens 37:2313–2337

Kawamura M, Jayamana S, Tsujiko Y (1996) Relation between social and environmental conditions in Colombo Sri Lanka and the urban index estimated by satellite remote sensing data. Int Arch Photogramm Remote Sens 31:321–326

Kayet N, Pathak K, Chakrabarty A, Sahoo S (2016) Spatial impact of land use/land cover change on surface temperature distribution in Saranda Forest, Jharkhand. Model Earth Syst Environ 2:127. https://doi.org/10.1007/s40808-016-0159-x

Khan A, Chatterjee S (2016) Numerical simulation of urban heat island intensity under urban–suburban surface and reference site in Kolkata, India. Model Earth Syst Environ 2:71. https://doi.org/10.1007/s40808-016-0119-5

Kim K-H, Pauleit S (2007) Landscape character, biodiversity and land use planning: the case of Kwangju City Region, South Korea. Land Use Policy 24:264–274

Legates DR, McCabe GJ (1999) Evaluating the use of goodness-of-fit measures in hydrologic and hydroclimatic model validation. Water Resour Res 35(1):233–241

Legates DR, McCabe GJ (2012) A refined index of model performance: a rejoinder. Int J Climatol 33(4):1053–1056

Liu HQ, Huete A (1995) A feedback based modification of the NDVI to minimize canopy background and atmospheric noise. IEEE Trans Geosci Remote Sens 33(2):457–465

Mallick J, Kant Y, Bharath BD (2008) Estimation of land surface temperature over Delhi using Landsat-7 ETM+. J Ind Geophys Union 12(3):131–140

Mmom PC, Nwagwu FW (2013) Analysis of landuse and landcover change around the City of Port Harcourt, Nigeria. Glob Adv Res J Geogr Reg Plan 2(5):076–086

Musa J, Bako MM, Yunusa MB, Garba IK, Adamu M (2012) An assessment of the impact of urban growth on land surface temperature in FCT, Abuja using geospatial technique. Sokoto J Soc Sci 2:2

Mushore TD, Odindi J, Dube T, Mutanga O (2017) Prediction of future urban surface temperatures using medium resolution satellite data in Harare metropolitan city. Zimb Build Environ 122:397–410. https://doi.org/10.1016/j.buildenv.2017.06.033

Nie Q, Man W, Li Z, Huang Y (2016) Spatio-temporal impact of Urban impervious surface on land surface temperature in Shanghai, China. Can J Remote Sens 42(6):680–689. https://doi.org/10.1080/07038992.2016.1217484

Ogunjobi KO, Daramola MT, Akinsanola AA (2018) Estimation of surface energy fluxes from remotely sensed data over Akure, Nigeria. Spat Inf Res 26(1):77–89. https://doi.org/10.1007/s41324-017-0149-8

Ord JK, Getis A (1995) Local spatial autocorrelation statistics: distributional issues and an application. Geogr Anal 27(4):286–306

Pal S, Ziaul SK (2017) Detection of land use and land cover change and land surface temperature in English Bazar urban centre. Egypt J Remote Sens Space Sci 20:125–145

Qiao Z, Tian G, Xiao L (2013) Diurnal and seasonal impacts of urbanization on the urban thermal environment: a case study of Beijing using MODIS data. ISPRS J Photogramm Remote Sens 85:93–101

Ramachandra TV, Kumar U (2004) Geographic resources decision support system for land use, land cover dynamics analysis. In: Proceedings of the FOSS/GRASS Users Conference, Bangkok, 12–14 September 2004

Rizwan AM, Dennis LY, Chunho LIU (2008) A review on the generation, determination and mitigation of Urban Heat Island. J Environ Sci 20(1):120–128

Rose S, Peters NE (2001) Effects of urbanization on streamflow in the Atlanta area (Georgia, USA): a comparative hydrological approach. Hydrol Process 15:1441–1457

Rosenzweig C, Solecki W, Slosberg R (2006) Mitigating New York City's heat island with urban forestry, living roofs, and light surfaces. A report to the New York State Energy Research and Development Authority

Sahana M, Ahmed R, Sajjad H (2016) Analyzing land surface temperature distribution in response to land use/land cover change using split window algorithm and spectral radiance model in Sundarban Biosphere Reserve, India. Model Earth Syst Environ 2:81. https://doi.org/10.1007/s40808-016-0135-5

Sannigrahi S, Rahmat S, Chakraborti S, Bhatt S, Jha S (2017) Changing dynamics of urban biophysical composition and its impact on urban heat island intensity and thermal characteristics: the case of Hyderabad City, India. Model Earth Syst Environ 3:647. https://doi.org/10.1007/s40808-017-0324-x

Sterling S, Ducharne A (2008) Comprehensive data set of global land cover change for land surface model applications. Global Biogeochem Cycles 22:GB3017. https://doi.org/10.1029/2007GB002959

Tucker CJ (1979) Red and photographic infrared linear combinations for monitoring vegetation. Remote Sens Environ 8:127–150

United Nations (2012) World Urbanization Prospects: the 2011 revision, United Nations Department of Economic and Social Affairs, Population Division, New York

Wang Z, Gang C, Li X, Chen Y, Li J (2015) Application of a normalized difference impervious index (NDII) to extract urban impervious surface features based on Landsat TM images. Int J Remote Sens 36(4):1055–1069. https://doi.org/10.1080/01431161.2015.1007250

Willmott CJ, Robeson SM, Matsuura K (2012) A refined index of model performance. Int J Climatol 32:2088–2094. https://doi.org/10.1002/joc.2419

Xu H (2008) A new index for delineating built-up land features in satellite imagery. Int J Remote Sens 29:4269–4276

Yuan F, Bauer ME (2007) Comparison of impervious surface area and normalized difference vegetation index as indicators of surface urban heat island effects in Landsat imagery. Remote Sens Environ 106(3):375–386

Zha Y, Gao J, Ni S (2003) Use of normalized difference built-up index in automatically mapping urban areas from TM imagery. Int J Remote Sens 24(3):583–594

Zhang X, Zhong T, Feng X, Wang E (2009) Estimation of the relationship between vegetation patches and urban land surface temperature with remote sensing. Int J Remote Sens 30(8):2105–2118. https://doi.org/10.1080/01431160802549252

Zhang Y, Odeh IOA, Ramadan E (2013) Assessment of land surface temperature in relation to landscape metrics and fractional vegetation cover in an urban/peri-urban region using Landsat data. Int J Remote Sens 34(1):168–189. https://doi.org/10.1080/01431161.2012.712227